AIAA '89

AIAA 89-0050
Structure of the Near-Injector Region of Non-Evaporating Pressure-Atomized Sprays

G. Ruff, L. Bernal and G. Faeth, Univeristy of Michigan, Ann Arbor, MI

27th Aerospace Sciences Meeting

January 9–12, 1989/Reno, Nevada

STRUCTURE OF THE NEAR-INJECTOR REGION OF NON-EVAPORATING PRESSURE-ATOMIZED SPRAYS

AIAA-89-0050

by

G. A. Ruff*, L. P. Bernal† and G. M. Faeth§
Department of Aerospace Engineering
The University of Michigan, Ann Arbor, Michigan

Abstract

The dense-spray region of pressure-atomized nonevaporating sprays in the atomization breakup regime was studied, emphasizing the properties of the multiphase mixing layer which surrounds the all-liquid core. The dispersed-phase properties of a large-scale (9.5 mm injector diameter) water jet injected vertically down in still air was measured using double-flash holography. The inner portion of the mixing layer contained large irregularly-shaped liquid elements and drops with the proportion of drops increasing and drop sizes decreasing with increasing radial distance. The all-liquid core and the liquid elements cause mean liquid volume fractions to be high near the axis; however, the gas-containing region is relatively dilute at each instant. The velocities of large drops are generally much larger than small drops and predictions based on the locally-homogeneous-flow approximation, providing direct evidence of significant separated-flow effects. Thus, the locally-homogeneous-flow approximation only provided good estimates of mixing properties for liquid volume fractions greater than 0.2 during past studies because the small drops and the gas contribute very little to the dynamics of the flow due to their small mass fractions at these conditions, not because their motion satisfies the locally-homogeneous-flow approximation.

Nomenclature

d	= injector diameter
d_{max},d_{min}	= maximum and minimum diameters of liquid elements
d_p	= drop or liquid element effective diameter
e_p	= drop or liquid element effective ellipticity
f	= mixture fraction
k	= turbulence kinetic energy
L	= injector passage length
Oh	= Ohnesorge number, $\mu_f/(\rho_f d\sigma)^{1/2}$
r	= radial distance
Re	= Reynolds number, $\rho_f u_o d/\mu_f$
SMD	= Sauter mean diameter
u	= streamwise fluid velocity
u_p	= streamwise drop velocity
v	= radial fluid velocity
w	= tangential fluid velocity
We_i	= Weber number of phase i, $We_i = \rho_i u_o^2 d/\sigma$
x	= streamwise distance
α	= volume fraction
ε	= rate of dissipation of turbulence kinetic energy
μ	= molecular viscosity
ρ	= density
σ	= surface tension
ϕ	= generic property

Subscripts

c	= centerline value
f	= liquid-phase property
g	= gas-phase property
o	= injector exit condition
∞	= ambient property

Superscripts

$(\bar{})$,$(\bar{})'$	= time-averaged mean and root-mean-squared fluctuating quantities
$(\tilde{})$,$(\tilde{})''$	= Favre-averaged mean and root-mean-squared fluctuating quantities

Introduction

This investigation considered the near-injector, dense-spray, region of nonevaporating pressure-atomized sprays, e.g., round water jets injected into still air. The flow is of interest as the multiphase counterpart of the single-phase round turbulent jet; however, it also has numerous practical applications in propulsion and power systems, e.g., pressure atomization is used for fuel or propellant injectors of afterburners, liquid rocket engines, and fuel-injected internal combustion engines. Earlier measurements of liquid volume fractions and entrainment rates in the dense-spray region, reported by Ruff et al.,[1] were extended to provide the properties of the dispersed phase using single- and double-flash holography. The new measurements were used to continue evaluation of analysis of the flow based on the locally-homogeneous-flow (LHF) approximation of multiphase flow theory, i.e., the assumption that interphase transport rates are infinitely fast so that both phases have the same instantaneous velocity and are in thermodynamic equilibrium at each point in the flow. Present considerations were limited to the near-injector region, within the atomization breakup regime as defined by Ranz,[2] since this breakup regime is of greatest importance for practical applications.

Figure 1 is a sketch of the near-injector region of a pressure-atomized spray during atomization breakup.[3] The near-injector region involves an all-liquid core surrounded by a multiphase mixing layer which begins to develop right at the injector exit for atomization breakup. The portion of the multiphase mixing layer nearest to the all-liquid core is a complex flow — containing irregular liquid elements, ligaments and drops — which results from the removal of liquid from the core as the first step in the atomization process. The outer edge of the mixing layer, however, has characteristics similar to a dilute spray, consisting of rather widely spaced spherical drops with mean liquid volume fractions less than 1 percent. The boundary between the dense- and dilute-spray regions is not well defined; however, most studies of dilute sprays have been limited to the region downstream of the all-liquid core as identified in Fig. 1. The resulting dense-spray region can extend quite far from the injector, e.g., all-liquid cores are still present 200-400 injector diameters from the jet exit for injection into gases at atmospheric pressure. Furthermore, the dense-spray region establishes initial conditions of the flow as it enters the dilute-spray region. Thus, processes within dense sprays have a very important influence on the structure and mixing properties of sprays.

* Graduate Assistant.
† Assistant Professor.
§ Professor, Fellow AIAA.

Past studies of dense sprays have recently been reviewed by Faeth;[3] therefore, only their main features will be considered here. Earlier work has been relatively limited due to the difficulties of making measurements, or even optically penetrating, a multiphase flow when liquid volume fractions vary over a wide range Thus, even the extent of the dense-spray region is uncertain. Phinney,[4] Hiroyasu et al.,[5] and Chehroudi et al.[6] have attempted to measure the length of the all-liquid core; however, their results are scattered and are not in good agreement with one another.[6]

In an attempt to circumvent the difficulties of treating the details of a flow having widely varying phase topography and a variety of physical phenomena — collisions, breakup, interphase transport with closely-packed dispersed-phase elements, etc. — a number of workers have studied the use of the LHF approximation to analyze dense sprays. LHF analysis circumvents the need for separated-flow parameters that are poorly understood for dense sprays, however, the effectiveness of the approach is controversial. Bracco,[7] and Wu et al.[8,9] report measurements of spray angles and drop velocities in nonevaporating pressure-atomized sprays at high pressures, concluding that LHF analysis was effective for their test conditions. On the other hand, earlier work in this laboratory indicated that the LHF approach generally overestimates the rate of development of multiphase jets and while it provides useful qualitative information it is not quantitatively accurate for most practical sprays.[10-17] Even results of LHF analysis for sprays in high-pressure gases were not satisfactory since drop inertia is significant in the rapidly decelerating flow field of typical sprays due to relatively small injector diameters and fast rates of entrainment.[10,11] Experimental evidence on both sides of the controversy comes from dilute portions of sprays and particle-laden flows, however, and the relevance of this information to dense-spray processes is questionable.

The first phase of the present investigation sought to help resolve controversies concerning the structure and extent of the dense-spray region, and the effectiveness of analysis of dense sprays based on the LHF approximation.[1] Experiments were undertaken with large-scale (9.5 and 19.1 mm diameter injectors having both fully-developed and slug flows at the injector exit) non-evaporating water jets in still air at atmospheric pressure. Operation in both the wind-induced and atomization breakup regimes was considered. The following measurements were made: flow visualization using flash photography, time-averaged mean liquid volume fractions using gamma-ray absorption, and air entrainment rates and mean and fluctuating liquid velocities at the jet exit using laser-Doppler anemometry (LDA). Measurements were compared with predictions based on the LHF approximation along the lines of Mao et al.,[10,11] after calibration of estimates of turbulent mixing rates based on measurements in single-phase variable-density jets.[3]

The findings of Ruff et al.[1] have helped to clarify some issues of dense sprays. Measurements of mean liquid volume fractions showed that the initial rate of development of the flow, and the length of the all-liquid core, are strongly dependent on both the degree of flow development at the jet exit and the breakup regime, with fully-developed flow and atomization breakup yielding the fastest rates of flow development. This sensitivity of the flow to jet exit conditions probably accounts for past controversies concerning the length of the all-liquid core,[4-6] since it is difficult to provide well-defined jet exit conditions when small injector passages are used. Predictions of mean liquid volume fractions based on the LHF approximation were reasonably good within the near-injector region for atomization breakup, including correct predictions of the sensitivity of the flow to the degree of flow development at the jet exit. However, predictions began to significantly overestimate the rate of development of the flow as the spray became dilute, i.e. for mean liquid volume fractions along the axis less than 0.2. Furthermore, the theory provided no warning of vastly reduced mixing rates that were observed when the flow was in the wind-induced breakup regime, where formation of the multiphase mixing layer begins downstream of the jet exit and drop sizes are generally larger than for atomization breakup. Finally, entrainment rates of the sprays were generally overestimated for all conditions, although predictions tended to improve as Reynolds numbers were increased in the atomization breakup regime. This behavior was attributed to the poorer performance of LHF analysis in dilute sprays since entrainment is dominated by the mixing properties of the dilute-spray region near the outer edge of the multiphase mixing layer. The findings generally suggested that the LHF approximation represents behavior approaching the limit of infinitely-large jet Reynolds numbers or Ohnesorge numbers,[18,19] where drops become infinitely small; concluding that practical sprays invariably involve effects of separated flow — particularly in the dilute-spray regions of the flow.

The present investigation extends the study of Ruff et al.,[1] emphasizing separated-flow phenomena within the multiphase mixing layer near the injector exit. Measurements were carried out using the same apparatus with test conditions limited to the atomization breakup regime. Visualization of the flow was emphasized in order to provide direct information on the topography of the dispersed phase within the multiphase mixing layer. This was accomplished using single- and double-flash holography to yield drop size and velocity distributions as well as the character of irregular liquid elements found near the all-liquid core. Similar to Ruff et al.,[1] measurements were compared with predictions based on the LHF approximation to help provide a measure of separated-flow effects.

The paper begins with a description of experimental methods followed by discussion of the main features of the LHF analysis. The paper concludes with a description of experimental findings, considering the appearance of the flow, drop and liquid element sizes, and drop velocities within the multiphase mixing layer. The present discussion is brief, additional details can be found in Ruff et al.[20] and Parthasarathy et al.[21]

Experimental Methods

Apparatus

Based on measurements of drop size distributions in dilute sprays, an effect of injector diameter on dense spray properties can be anticipated but it is not strong.[22] Thus, a large-scale (9.5 mm injector diameter) jet was used in order to get adequate spatial resolution for observations. Figure 2 is a sketch of the experimental arrangement. Water was used as the test liquid, injected vertically downward in still air. The water was collected in a baffled tub, to prevent splashing up into the area where measurements were made, and discharged to a drain. City water was supplied to the injector by a centrifugal pump. The water flow rate was adjusted using a bypass system and measured with a turbine flow meter which was calibrated by collecting water for timed intervals.

Present tests were limited to a long length-to-diameter injector which provided fully-developed turbulent pipe flow at the injector exit. The injector consisted of a honeycomb flow straightener (1.6 mm cells, 25 mm long) followed by a simple circular converging section to a constant-area passage having a length of 41 passage diameters. Measurements of distributions of mean and fluctuating velocities at the injector exit[20] were in reasonably good agreement with existing measurements for fully-developed turbulent pipe flow.[23,24] Instrumentation was mounted rigidly; therefore, the flow structure was measured by traversing the injector horizontally (up to 1m with a positioning accuracy of 5 μm) and vertically (up to 2m with a positioning

accuracy of 0.5 mm).

Instrumentation

Earlier measurements involving flow visualization using flash photography, liquid volume fractions using gamma-ray absorption, and jet exit and entrainment velocities using laser Doppler anemometry are described elsewhere.[1,20,21] Present measurements were limited to dispersed-phase properties in the multiphase mixing layer using holography.

Since the topography of liquid elements in dense sprays is variable, direct photography provides the only reliable approach for measuring dispersed-phase properties. The combined requirements of high magnification, reasonable depth of field, and analysis of non-planar motion, can best be satisfied by single-flash holography for liquid element size and shape properties, and double-flash holography for liquid element velocities. An off-axis holographic arrangement was used based on the Spectron Development Laboratories Model HTRC-5000 system, with an angle of 28° between the object and reference beams. The system was modified, however, to improve performance in dense sprays. In particular, dense sprays require large light intensities so that the flow can be penetrated, and high magnification since small drops are of interest. This was accomplished by reducing the diameter of the object beam through the spray and then subsequently expanding it (7-8:1) back to the same size as the reference beam (85 mm diameter) when the two signals were optically mixed to form a hologram. The reference beam was directed past the spray within a 300 mm diameter tube to reduce optical noise from small drops in the environment caused by the spray collection system. The holograms were produced using a ruby laser that deposited 50 mJ in roughly 20 ns. The short laser pulse time stopped the motion adequately so that drops as small as 2 μm in diameter could be observed and drops as small as 5 μm in diameter could be measured. The laser could be double pulsed with pulse separation times as short as 3 μs. This yielded holograms that could be reconstructed to show the object field at two instants of time, providing a means of measuring liquid element velocities. The holograms were obtained in a darkened room using AGFA 8F25HD-NAH unbacked holographic film plates with a 100 × 125 mm film format.

The holograms were reconstructed using a 15 mW cw HeNe laser which was expanded to 60 mm diameter and then passed through the developed hologram to provide a real image of the spray in front of the hologram. The properties of the reconstructed spray were observed with an MTI Model 65 video camera with optics that provided fields of view of roughly 1 × 1.2 mm and 2.5 × 3 mm. The larger field of view was more convenient for analyzing ligaments and other large liquid elements due to its greater depth-of-field. Computer controlled x-y traversing of the hologram (with a 1 μm resolution) and z traversing of the video camera (with 5 μm resolution) allowed the region crossed by the object beam to be studied. The video image was analyzed using a Gould FD 5000 Image Processing System. A system of pins near the edge of the region being studied provided size and position reference points on the reconstructed image of the spray.

Drops and other more-or-less ellipsoidal-shaped liquid elements were sized by finding the maximum and minimum diameter through the centroid of the image. Assuming that the liquid element was ellipsoidal, its diameter was taken to be the diameter of an ellipsoid having the same volume, i.e., $d_p^3 = d_{min}^2 d_{max}$. The shape of the element was characterized by its ellipticity, defined as $e_p = d_{max}/d_{min}$. This approach was not appropriate for elongated liquid elements or ligaments where the centroid of the image often fell outside the boundaries of the image or where there were several necked-in points along the length of the element. In these cases, the cross-sectional area and perimeter of the image were measured and the maximum and minimum diameters of an ellipsoid having the same cross-sectional area and perimeter were computed. Given these parameters the effective diameter and ellipticity were calculated in the same manner as for drops. Results at each position in the flow were summed to find the Sauter mean diameter (SMD) and the volume-averaged ellipticity.

Velocity measurements were limited to drops and more-or-less ellipsoidal-shaped liquid elements since it was difficult to obtain non-overlapping images of larger objects having complex shapes. These measurements were based on the motion of the centroid of the image and were correlated as a function of diameter using a least-squares fit. This allowed plots of drop velocities at fixed diameters across the width of the mixing layer while making maximum use of data on the holograms at each position.

Measurements were made at x/d = 12.5, 25, 50 and 100 for r/x = 0.050, 0.075, 0.100, 0.125 and 0.150 except in instances where the innermost location was still within the all-liquid core. Measurements at each location were obtained from a 4 × 4 × 4 mm volume, averaging results over no less than four holograms. This corresponds to a spatial average of ± r/x = 0.017 at x/d = 12.5, reduced proportionally at larger distances from the injector exit. Measurements involved analysis of 50-100 objects for $r/x \leq 0.075$ and 200-500 objects for $r/x \geq 0.100$, the fewer objects nearer the liquid core reflecting the fact that liquid elements were generally much larger in this region.

Experimental uncertainties were generally dominated by sampling limitations rather than the resolution of liquid element properties from the reconstructed holograms. Estimates of experimental uncertainties (95 percent confidence) are as follows: Sauter mean diameter less than 10 percent, volume-averaged ellipticity less than 15 percent, and liquid element velocities less than 20 percent.

Test Conditions

Measurements of the structure of the multiphase mixing layers were limited to fully-developed jet exit conditions for atomization breakup using a 9.5 mm diameter injector passage. The test conditions are summarized in Table 1. The injector Reynolds number was reasonably high yielding nearly fully-developed turbulent pipe flow at the jet exit. Ranz[2] suggests $We_f > 8$ and $We_g > 13$ for atomization breakup, while Miesse[25] recommends $We_g > 40.3$ for atomization breakup: by either criterion the present flow was well into the atomization breakup regime which clearly corresponded to its appearance.[1]

Table 1 Summary of Test Conditions[a]

Injector diameter (mm)	9.5
Flow rate (kg/s)	3.99
Injector pressure drop (kPa)	2520
u_o (m/s)[b]	56.7
Re	534000
We_f	419000
We_g	492.8
Oh	0.00121

[a] Pressure-atomized water jet injected vertically downward in still air at 98.8 kPa, 298 ± 2K, L/d = 41; yielding fully-developed turbulent pipe flow at injector exit and atomization breakup.

[b] Average jet exit velocity.

Theoretical Methods

Analysis of the dense spray was limited to the use of the LHF approximation along the lines of past work in this laboratory, see Faeth[3] for a description of the general formulation. The main features of the analysis will be described in the following, however, since the formulation was simplified in the interest of reducing empiricism from the approach described by Ruff et al.[1] and Ruff and Faeth[20] for the same flows. In particular, it was found that the low levels of water evaporation in the test sprays had little effect on predictions;[1] therefore, this effect was ignored, passing to the limit of a nonevaporating spray.

In addition to the LHF approximation, the major assumptions of the analysis were as follows: steady (in the mean) axisymmetric flow with no swirl; boundary-layer approximations apply; negligible kinetic energy and viscous dissipation of the mean flow; buoyancy only affects the mean flow; equal exchange coefficients of all species and phases; and negligible mass transport between the phases. These assumptions are either conditions of the experiments or have been justified by in the past, with the exception of the LHF approximation which is to be evaluated here.

Under these assumptions, all scalar properties are only functions of mixture fraction (defined as the fraction of mass at a point which originated from the injector). Furthermore, the instantaneous mixture fraction can only take on values of 0 or 1 since a particular point can only be in either gas (f=0) or liquid (f=1), i.e., the probability density function of mixture fraction consists of Dirac delta functions at f=0 and 1. Denoting scalar properties at the jet exit and in the environment to be ϕ_o and ϕ_∞, all mean scalar properties can then be found in terms of the Favre averaged mean mixture fraction, $\tilde{f}$, as follows:

$$\tilde{\phi} = \phi_\infty(1 - \tilde{f}) + \phi_o\tilde{f} \qquad (1)$$

$$\bar{\phi} = (\phi_\infty\rho_o(1 - \tilde{f}) + \phi_o\rho_\infty\tilde{f})/(\rho_{o\,(1\,-\,\tilde{f})} + \rho_\infty\tilde{f}) \qquad (2)$$

Similarly, higher moments of scalars — $\tilde{\phi}''$, $\bar{\phi}'$, etc. — are also only functions of $\tilde{f}$ for present conditions.

Given Eqs. (1) and (2), the flow field can be found using a simplified version of the conserved-scalar formalism of Lockwood and Naguib,[26] but based on mass-weighted (Favre) averages, following Bilger.[27] Governing equations are solved for conservation of mass, streamwise mean momentum, mean mixture fraction, turbulence kinetic energy, and the rate of dissipation of turbulence kinetic energy. Unlike the formulation of Ruff et al.[1] and Ruff and Faeth[20] (which is suitable for evaporating flow), however, there is no need to solve a governing equation for mean-squared mixture fraction fluctuations since scalar properties can be found in terms of $\tilde{f}$ from Eqs. (1) and (2). The specific formulation of the governing equations and all empirical constants can be found in Ref. 3. The approach was successfully calibrated for a variety of constant and variable density single-phase round jets;[28] the formulation and constants, however, are not very different from those used by Lockwood and Naguib.[26]

Initial conditions for the calculations were specified at the injector exit. The LDA velocity measurements showed that flow properties closely approximated fully-developed turbulent pipe flow; therefore, rather than interpolate LDA measurements at x/d = 0.1, initial profiles of $\tilde{u}$, k and ε were taken from Hinze[23] and Schlichting[24] for fully-developed turbulent pipe flow while $\tilde{f}$ = 1 at the injector exit by definition (note that Favre- and time-averaged quantities are identical for the single-phase flow at the injector exit).

The governing equations were solved using GENMIX.[29] The large density variation of the flow caused problems of computational stability and numerical accuracy, requiring much finer grids than are usually needed for single-phase flows. Present computations used 720 crosstream grid nodes with streamwise step sizes limited to 0.15 percent of the current flow width. Doubling the number of grid nodes in both the crosstream and streamwise directions changed predictions less than 1 percent.

Results and Discussion

Flow Visualization

Photographs of typical hologram reconstructions, taken from the video monitor of the image analysis system, are illustrated in Figs. 3-5. These results were obtained within the multiphase mixing layer at x/d = 12.5 and r/x = 0.150, 0.100 and 0.075. These radial positions correspond to points near the outer edge of the multiphase mixing layer, near the middle of the multiphase mixing layer, and near the all-liquid core, respectively. All three photographs were obtained with the same magnification yielding a field of view of 1725 × 2250 μm and are from single-pulse holograms. Except near the liquid surface, usually only a few drops or liquid elements (or portions of them) are in focus for any one screen image of the video monitor. Thus, the photographs have a mottled appearance due to out-of-focus drops. Furthermore, the images on the monitor are much larger and easier to interpret — particularly since the focal plane can be moved to sharpen the focus on any one object.

Conditions near the outer edge of the multiphase mixing layer, Fig. 3, correspond to a dilute spray: the liquid elements consist of relatively small spherical drops and the liquid volume fraction is quite small so that the drops are spaced quite far from one another. Moving to the middle of the multiphase mixing layer, Fig. 4, the flow largely remains a dilute spray although drop diameters and drop number densities are larger than near the edge of the flow. In this region, however, some of the larger liquid elements are no longer spherical although the ellipticities of individual liquid elements are rarely greater than 2. Finally, as the edge of the all-liquid core is approached, Fig. 5, the liquid elements become quite large and are generally very irregular in shape, consisting of ligaments and oblong ellipsoids surrounded by only a few spherical drops. The lower right-hand corner of Fig. 5 actually corresponds to a section of the surface of the all-liquid core. This surface is quite irregular and involves long liquid elements protruding into the mixing layer, suggesting initial growth of ligaments before they break away from the surface. A surprising feature of the region near the liquid core, however, is that the gas-containing region is relatively dilute at each instant. Even high-magnification reconstructions of this region did not reveal large numbers of small drops. Thus the main difference between the dilute- and dense-spray regions of the multiphase mixing layer is that the dense-spray region contains large and irregular liquid elements, including protuberances from the all-liquid core. These large liquid objects, as well as lateral fluctuations of the all-liquid core itself, cause time-averaged liquid volume fractions to be large even though the gas-containing region surrounding the liquid elements is relatively dilute at each instant.

Flow Structure

Measurements of flow structure within the multiphase mixing layer for x/d = 12.5, 25, 50 and 100 are illustrated in Figs. 6-9. The volume-averaged ellipticity, the SMD and drop velocities for d_p = 10, 30 100 and 300 μm, are plotted as a function of r/x, which is the radial similarity variable for

turbulent single-phase jets and plumes. This radial similarity variable has only been chosen for convenience: the region considered is analogous to the mixing-layer around the potential core of a single-phase jet due to the presence of the all-liquid core; therefore, radial profiles for flow properties do not exhibit similarity in the r/x coordinate system. The measurements extend from near the edge of the all-liquid core (which was observed at r/x = 0.068-0.076 and 0.047-0.063 for x/d = 12.5 and 25 in Figs. 6 and 7), to near the outer edge of the multiphase flow region, r/x ca. 0.150.

In Figs. 6-9, large values of volume-averaged ellipticity, which are associated with the presence of large and irregular liquid elements, are generally found in the region of the all-liquid core. This region extends across most of the multiphase mixing layer near the jet exit but becomes progressively confined to the region near the axis with increasing distance from the jet exit. Thus, the near-injector region of the spray can be divided into three regions: an all-liquid core, a dense-spray region characterized by nonunity ellipticities, and an outer dilute-spray region where ellipticities are near unity. The outer region progressively grows with increasing distance from the injector, eventually reaching the axis somewhat downstream of the region where liquid stripping by the formation of ligaments and other large liquid elements has caused the all-liquid core to disappear.

Sauter mean diameters, illustrated in Figs. 6-9, progressively decrease with increasing radial distance, similar to the ellipticity. Values of the SMD near the all-liquid core are quite large, 500-800 μm, due to the presence of large irregular liquid elements. Near the edge of the flow in the dilute-spray region, however, drop sizes are much smaller, in the range 100-200 μm. In a few positions, measurements are somewhat inconsistent with respect to neighboring points, e.g., results at r/x = 0.10 in Fig. 7. This behavior is probably due to sampling limitations: additional measurements are being obtained to reduce aberrations of this type. Several phenomena are probably responsible for the progressive reduction of SMD with increasing radial distance, as follows: the tendency of large liquid elements to shatter as they encounter low velocity gas near the edge of the flow; the fact that breakup of ligaments and other large liquid elements requires a finite time allowing them to traverse the inner portions of the mixing layer, and increased turbulent dispersion of small drops which enhances their migration toward the edge of the flow.

Distributions of drop velocities in Figs. 6-9 include both measurements for various drop diameters and predictions based on the LHF approximation. In the region near the all-liquid core, the largest drops have velocities which are comparable to liquid injection velocities, ca. 57 m/s. This follows since velocities within the all-liquid core remain relatively close to jet exit velocities while the large drops have probably only recently formed and have not had sufficient time for drag from the gas phase to slow their motion. The velocities of drops of all sizes, however, tend to decrease with increasing radial distance. This is expected since gas velocities are lowest near the edge of the flow and drops in this region have had more time to accommodate to gas velocities. A surprising feature of the results of Figs. 6-9, however, is that small drops (which should have velocities relatively close to local gas velocities) have relatively low velocities which are nearly constant across much of the mixing layer — particularly at x/d = 12.5 and 25 (Figs. 6 and 7). This suggests that momentum exchange between the liquid and gas is not very efficient in the multiphase mixing layer, perhaps due to the presence of large liquid elements (having relatively low surface-to-volume ratios) in the dense spray region near the all-liquid core. This results in relatively large relative velocities between the phases near the all-liquid core which probably helps promote breakup.

The fact that the drop velocities plotted in Figs. 6-9 vary substantially with drop diameter at each point in the flow provides direct evidence that use of the LHF approximation is not appropriate for the present flow. In view of this, it is hardly surprising that the LHF predictions are not in good agreement with the measurements. The nature of the failure is typical of past evaluation of the LHF approximation for dilute sprays; namely, the rate of development of the flow is overestimated since the analysis does not properly account for the inertia of large drops which take significant time to exchange momentum with the gas phase. In view of the results of Figs. 6-9, it is also not surprising that the LHF approach tended to overestimate the rate of entrainment of the flow during the evaluation of Ref. 1. Under the LHF approximation all of the momentum of the flow is available to the continuous phase to help promote mixing; however, since the drops have substantial relative velocities their relative momentum is not available to the gas phase and mixing is reduced accordingly.

Ruff et al.[1] observed that use of the LHF approximation provided reasonably good predictions of liquid volume fractions in the dense-spray portion of the present flow ($\bar{\alpha}_f$ > 0.2). In view of the velocity measurements of Figs. 6-9, which exhibit large differences in velocity between large drops and small drops (which should crudely approximate gas velocities) almost everywhere, it is clear that this agreement does not result from the LHF approximation being formally satisfied. A more likely explanation is that the dynamics of the flow are dominated by the large liquid elements so that even though the gas and small drops are moving at much lower velocities they do not have a significant effect. This follows since the mass fraction of gas and small drops is small due to the large density ratio of the flow (e.g., liquid volume fractions greater than 0.2 generally correspond to mixture fractions greater than 0.99) and the strong d_p^3 variation of drop mass with drop diameter.

Present measurements also do not support recent hypotheses concerning dense-spray structure which assume that small drops are either formed near the jet exit or are stripped from the surface of the all-liquid core and create larger drops within the multiphase mixing layer by collisions or coalescence.[7,30,31] Instead, it appears that large liquid elements like ligaments are formed along the surface of the all liquid core. These elements then break up into smaller liquid elements either due to the development of residual instabilities within the liquid elements which require additional time to complete their breakup action, or by the development of subsequent instabilities as the liquid elements pass through the relatively slow-moving gas. Smaller drops developed by breakup adjust more rapidly to local gas velocities so that the resulting reduced relative velocities, combined with larger relative stabilizing effects of surface tension, finally end the breakup process. The smaller drops then spread across the mixing layer through the mechanism of turbulent dispersion. Thus, dense sprays do not correspond to closely-spaced spherical elements dominated by collision processes; instead, they correspond to a relatively dilute flow of irregularly-shaped liquid elements dominated by breakup processes. Current estimates of breakup times of drops suggest that they are comparable to mixing times in sprays,[3] which appears to be consistent with present observations. Thus, it is likely that analysis of breakup will have to be an integral part of analysis of dense sprays. Fortunately, the fact that the dense-spray region is optically accessible using high-resolution holography should be helpful for gaining a better understanding of the breakup processes relevant to this flow.

Conclusions

The near-injector region of a pressure-atomized spray in the atomization breakup regime, with fully-developed turbulent pipe flow at the jet exit, was investigated. The major conclusions of the study are as follows:

1. Drop velocities increase significantly with increasing drop size throughout the near-injector region, providing unequivocal evidence of the importance of separated-flow effects in dense sprays. Thus, the success of the LHF approximation at high liquid volume fractions is largely caused by the fact that the momentum of the gas and small drops does not have a strong influence on the dynamics of the flow since their total momentum is a small fraction of the total due to the large density ratio of the flow, even though they have significantly different velocities from the bulk of the liquid.

2. The multiphase mixing layer around the all-liquid core primarily consists of large irregularly-shaped liquid elements and drops, near the core, with the proportion of drops increasing and drop sizes and mean liquid volume fractions decreasing with increasing radial distance. Even near the all-liquid core, however, the gas containing region is relatively dilute at each instant. This structure implies that breakup and turbulent dispersion of drops dominate processes in the multiphase mixing layer — not drop collisions as has been suggested in the past.

3. High resolution double pulse holography is capable of penetrating the multiphase mixing layer to the surface of the all-liquid core as long as the object beam is not directed through the all-liquid core itself. This instrument provides a valuable approach for studying the properties of dense sprays since it can deal with irregularly-shaped liquid elements that are problematical for other measurement techniques used in multiphase flows.

Acknowledgements

This research was sponsored by the Air Force Office of Scientific Research, Air Force Systems Command, USAF, under grant number AFOSR-85-0244. The U.S. Government is authorized to reproduce and distribute copies for Governmental purposes notwithstanding any copyright notation thereon.

References

[1]Ruff, G. A., Sagar, A. D. and Faeth, G. M., "Structure and Mixing Properties of Pressure-Atomized Sprays," AIAA Paper No. 88-0237, 1988; also, *AIAA J.*, in press.

[2]Ranz, W. E., "Some Experiments on Orifice Sprays," *Can. J. Chem. Engr.*, Vol. 36, August 1958, pp. 175-181.

[3]Faeth, G. M., "Mixing, Transport and Combustion in Sprays," *Prog. Energy Combust. Sci.*, Vol. 13, 1987, pp. 293-345.

[4]Phinney, R. E., "The Breakup of a Turbulent Liquid Jet in a Gaseous Atmosphere," *J. Fluid Mech.*, Vol. 60, October 1973, pp. 689-701.

[5]Hiroyasu, H., Shimizu, M. and Arai, M., "The Breakup of a High Speed Jet in a High Pressure Gaseous Environment," ICLASS-82, University of Wisconsin, Madison, Wisconsin, 1982.

[6]Chehroudi, B., Onuma, Y., Chen, S.-H. and Bracco, F. V., "On the Intact Core of Full-Cone Sprays," SAE Paper No. 850126, 1985.

[7]Bracco, F. V., Structure of High-Speed Full-Cone Sprays," *Recent Advances in Gas Dynamics* (C. Casci, ed.), Plenum Publishing Corp., New York, 1983.

[8]Wu, K.-J., Su, C.-C., Steinberger, R. L., Santavicca, D. A. and Bracco, F. V., "Measurements of the Spray Angle of Atomizing Jets," *J. Fluids Engr.*, Vol. 105, December 1983, pp. 406-415.

[9]Wu, K.-J., Coghe, A., Santavicca, D. A. and Bracco, F. V., "LDV Measurements of Drop Velocity in Diesel-Type Sprays," *AIAA J.*, Vol. 22, September 1984, pp. 1263-1270.

[10]Mao, C.-P., Wakamatsu, Y. and Faeth, G. M., "A Simplified Model of High Pressure Spray Combustion," *Eighteenth Symposium (International) on Combustion*, The Combustion Institute, Pittsburgh, 1981, pp. 337-347.

[11]Mao, C.-P., Szekely, G. A., Jr. and Faeth, G. M., "Evaluation of a Locally Homogeneous Flow Model of Spray Combustion," *J. Energy*, Vol. 4, March-April 1980, pp. 78-87.

[12]Shearer, A. J., Tamura, H. and Faeth, G. M., "Evaluation of a Locally Homogeneous Flow Model of Spray Evaporation," *J. Energy*, Vol. 3, September-October 1979, pp. 271-278.

[13]Solomon, A.S.P., Shuen, J.-S., Zhang, Q.-F. and Faeth, G. M., "Structure of Nonevaporating Sprays: I. Near-Injector Conditions and Mean Properties," *AIAA J.*, Vol. 23, October 1985, pp. 1548-1555.

[14]Solomon, A.S.P., Shuen, J.-S., Zhang, Q.-F. and Faeth, G. M., "Structure of Nonevaporating Sprays: II. Drop and Turbulence Properties," *AIAA J.*, Vol. 23, November 1985, pp. 1724-1730.

[15]Shuen, J.-S., Chen, L.-D. and Faeth, G. M., "Evaluation of a Stochastic Model of Particle Dispersion in a Turbulent Round Jet," *AIChE J.*, Vol. 29, January 1983, pp. 167-170.

[16]Shuen, J.-S., Chen, L.-D. and Faeth, G. M., "Predictions of the Structure of Turbulent, Particle-Laden, Round Jets," *AIAA J.*, Vol. 21, November 1983, pp. 1483-1484.

[17]Shuen, J.-S., Solomon, A.S.P., Zhang, Q.-F. and Faeth, G. M., "Structure of Particle-Laden Jets: Measurements and Predictions," *AIAA J.*, Vol. 23, March 1985, pp. 396-404.

[18]Reitz, R. D. and Bracco, F. V., "Mechanism of Atomization of a Liquid Jets," *Phys. Fluids*, Vol. 25, October 1982, pp. 1730-1742.

[19]Reitz, R. D., "Atomization and Other Breakup Regimes of a Liquid Jet," Ph.D. Dissertation No. 1375-T, Princeton University, Princeton, New Jersey, 1978.

[20]Ruff, G. A. and Faeth, G. M., "Dense-Spray Structure and Phenomena: Part II. Pressure-Atomized Sprays," Interim Report under Grant No. AFOSR-85-0244, The University of Michigan, Ann Arbor, Michigan, September 1987.

[21]Parthasarathy, R. N., Ruff, G. A., and Faeth, G. M., "Turbulence Modulation and Dense-Spray Structure," Annual Report under Grant No. AFOSR-85-0244, The University of Michigan, Ann Arbor, Michigan, August 1988.

[22]Lefebve, A. H., "Atomization," *Prog. Energy Combust. Sci.*, Vol. 6, 1980, pp. 223-246.

[23]Hinze, J. O., *Turbulence*, 2nd ed., McGraw-Hill, New York, 1975, p. 427 and pp. 724-734.

[24]Schlichting, H., *Boundary Layer Theory*, 7th ed., McGraw-Hill, New York, 1979, p. 599.

[25]Miesse, C. C., "Correlation of Experimental Data on Disintegration of Liquid Jets," *Ind. Engr. Chem.*, Vol. 47, September 1955, pp. 1690-1697.

[26]Lockwood, F. C. and Naguib, A. S., "The Prediction of Fluctuations in the Properties of Free, Round-Jet Turbulent Diffusion Flames," *Combust. Flame*, Vol. 24, February 1975, pp. 109-124.

[27]Bilger, R. W., "Turbulent Jet Diffusion Flames," *Prog. Energy Combust. Sci.*, Vol. 1, 1976, pp. 87-109.

[28]Jeng, S.-M. and Faeth, G. M., "Species Concentrations and Turbulence Properties in Buoyant Methane Diffusion Flames," *J. Heat Trans.*, Vol. 106, August 1985, pp. 721-727.

[29]Spalding, D. B., *GENMIX: A General Computer Program for Two-Dimensional Parabolic Phenomena*, Pergamon Press, Oxford, 1977.

[30]Reitz, R. D. and Bracco, F. V., "Mechanisms of Breakup of Round Liquid Jets," *Encyclopedia of Fluid Mechanics* (N. P. Cheremisinoff, ed.), Vol. III, Chapt. 11, 1984.

[31]Reitz, R. D. and Diwakar, R., "Structure of High-Pressure Fuel Sprays," SAE Paper No. 870598, 1987.

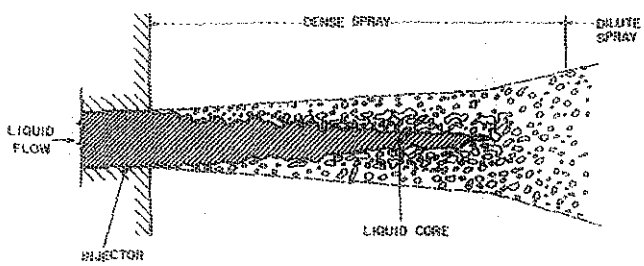

Fig. 1 Sketch of the dense-spray region.

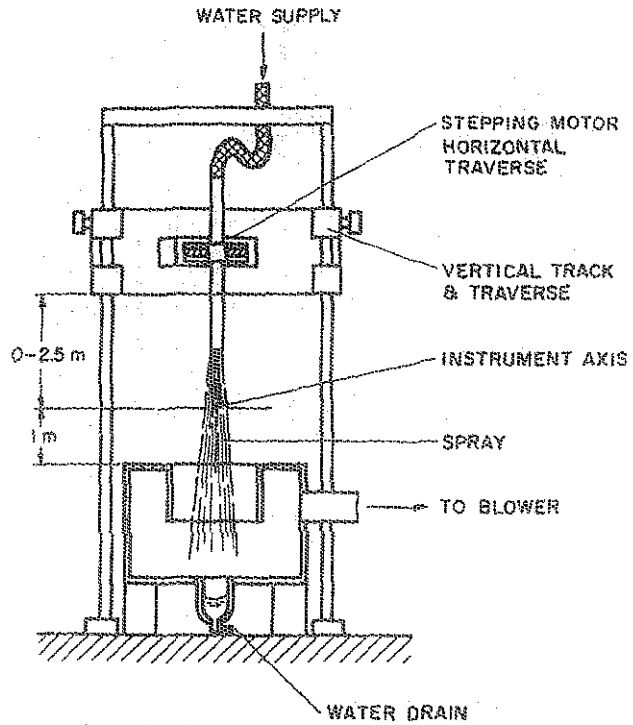

Fig. 2 Sketch of the test apparatus.

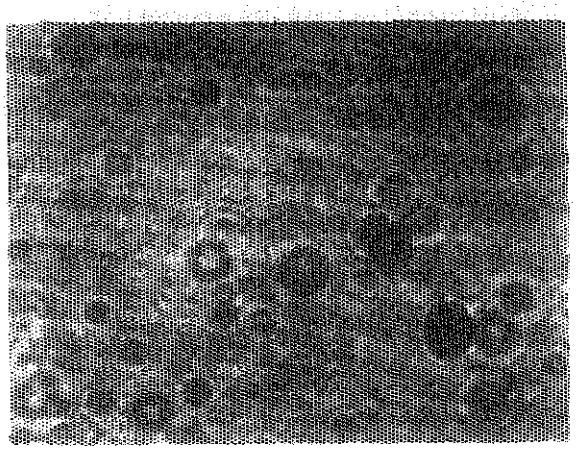

Fig. 3 Typical hologram reconstruction in the dense-spray region: x/d = 12.5, s/x = 0.150.

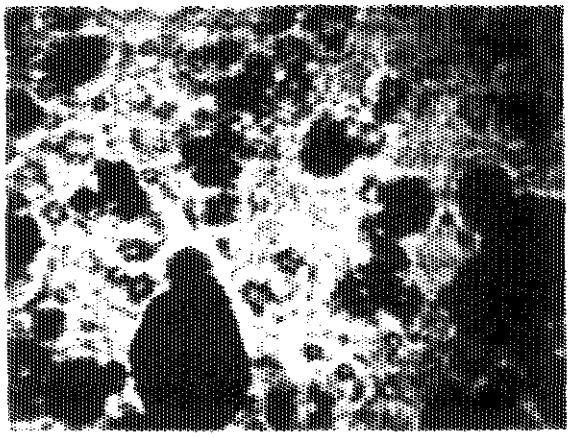

Fig. 4 Typical hologram reconstruction in the dense-spray region: x/d = 12.5, r/x = 0.100.

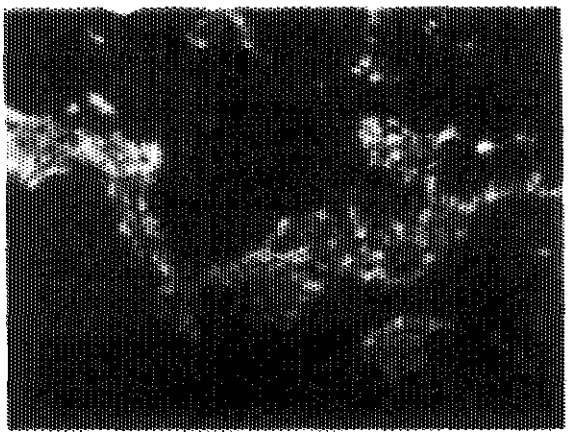

Fig. 5 Typical hologram reconstruction in the dense-spray region: x/d = 12.5, r/x = 0.075.

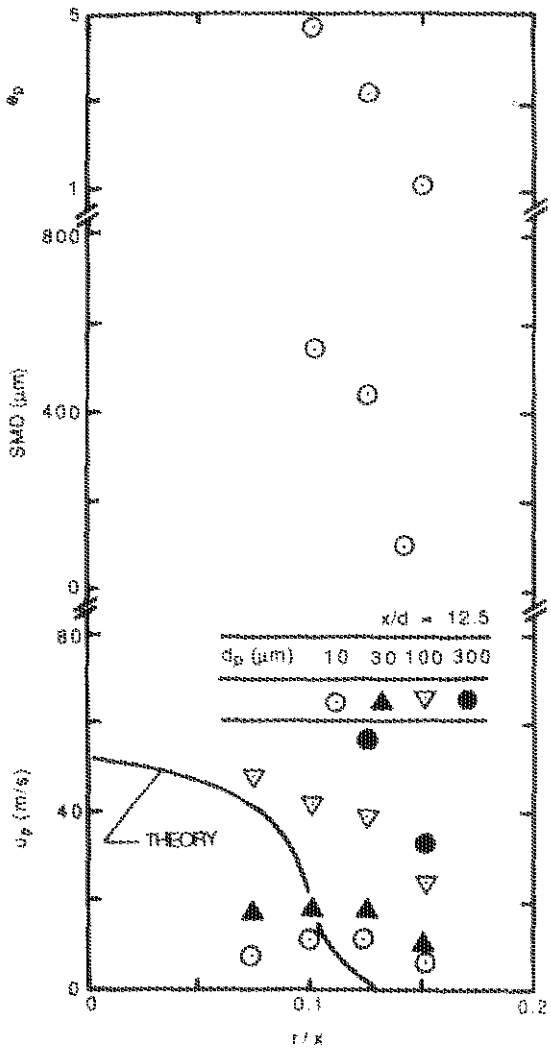

Fig. 6 Radial profiles of dispersed-phase properties at x/d = 12.5.

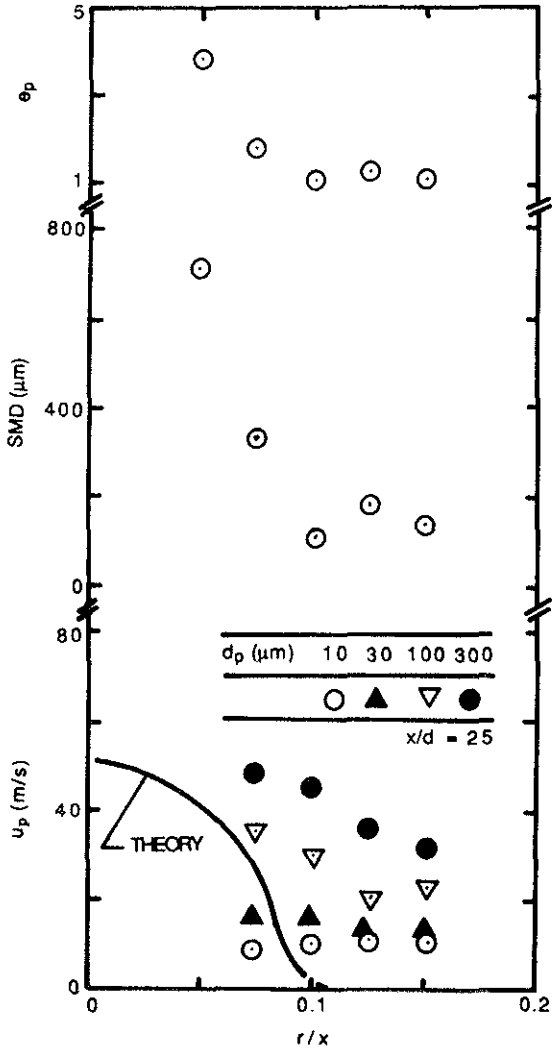

Fig. 7 Radial profiles of dispersed-phase properties at x/d = 25.

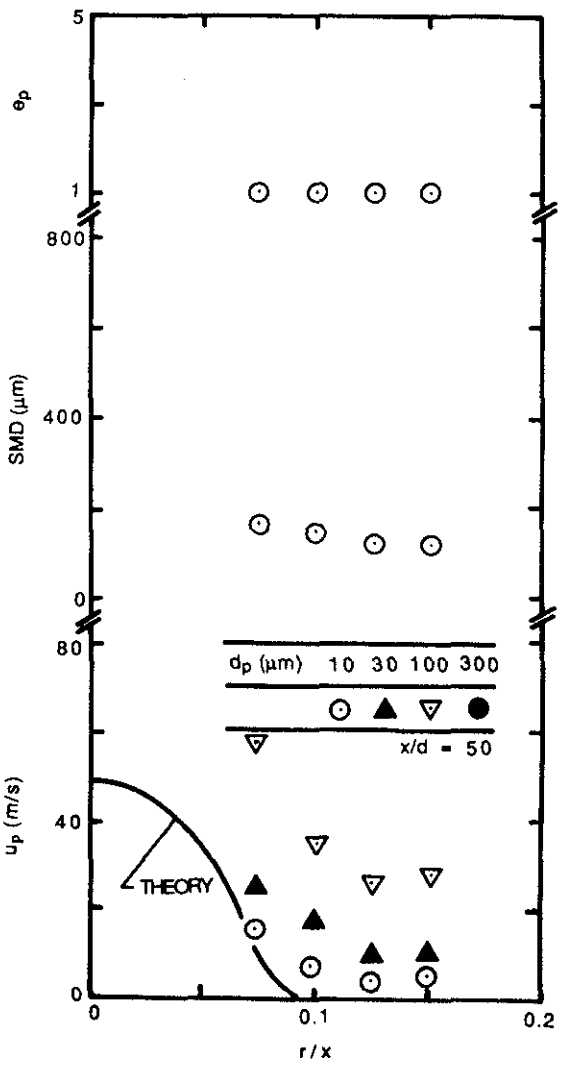

Fig. 8 Radial profiles of dispersed-phase properties at x/d = 50.

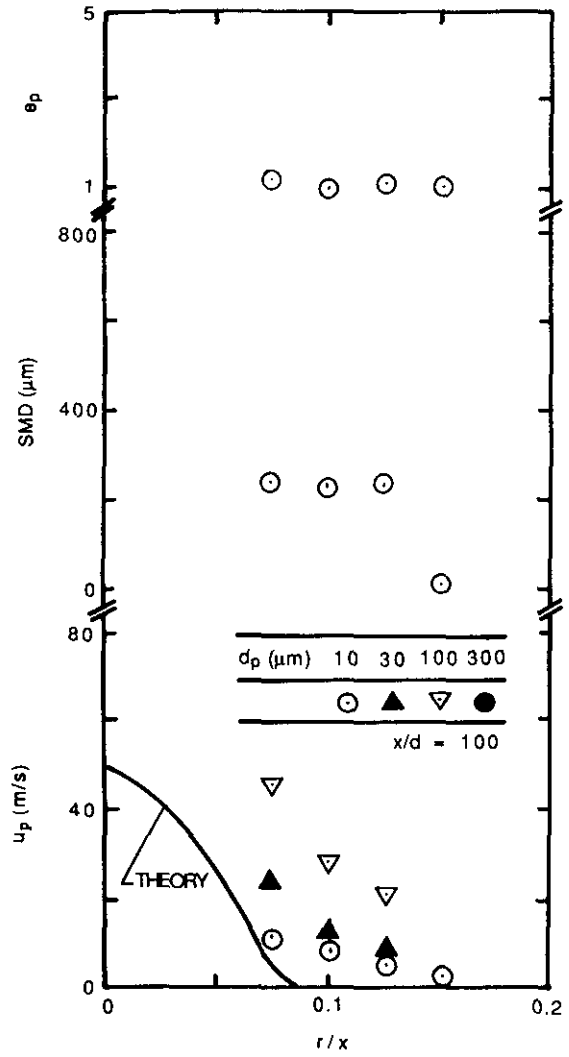

Fig. 9 Radial profiles of dispersed-phase properties at x/d = 100.